

process. This alternative perturbed equation involves the “score”, which is the gradient of the log of the instantaneous distribution of the system. While for most nonequilibrium systems the “score” cannot be computed analytically, recent progress in the machine learning literature on score-based diffusion models [16] and score estimation [17, 18] have led to new computational tools that provide arbitrarily precise score estimates, which would have previously seemed unobtainable. As we show analytically and numerically below, this transformed SDE gives excellent results for diffusion sensitivity on a variety of systems, including equilibrium, stationary nonequilibrium, and non-stationary nonequilibrium cases.

Computing diffusion sensitivities with the score-shifted SDE.— We consider a system with coordinates $\mathbf{x} \in \Omega \subset \mathbb{R}^d$ and represent the dynamics as an overdamped stochastic differential equation

$$d\mathbf{X}_t = \mathbf{b}(\mathbf{X}_t, t)dt + \sigma(\mathbf{X}_t, t)d\mathbf{W}_t, \quad (1)$$

where $\mathbf{b} : \mathbb{R}^d \times [0, T] \rightarrow \mathbb{R}^d$ is the drift, $\sigma : \mathbb{R}^d \times [0, T] \rightarrow \mathbb{R}^{d \times m}$ is a space and time-dependent mobility tensor, and \mathbf{W} is an m -dimensional Wiener process. We want to compute the *sensitivity* of an arbitrary, bounded, continuous observable $A \in \mathcal{C}_b^0(\Omega, \mathbb{R})$ to a perturbation to σ ,

$$\partial_{\tilde{\sigma}} A_t = \lim_{\epsilon \rightarrow 0} \epsilon^{-1} [\langle A(t) \rangle_{\epsilon} - \langle A(t) \rangle] \quad (2)$$

where $\langle \cdot \rangle$ denotes an expectation with respect to (1) and $\langle \cdot \rangle_{\epsilon}$ denotes an average with respect to the perturbed SDE,

$$d\mathbf{X}_t^{\epsilon} = \mathbf{b}(\mathbf{X}_t^{\epsilon}, t)dt + [\sigma(\mathbf{X}_t^{\epsilon}, t) + \epsilon \tilde{\sigma}(\mathbf{X}_t^{\epsilon}, t)]d\mathbf{W}_t. \quad (3)$$

The primary challenge when trying to compute a sensitivity of the type defined in (2) is that widely-used path reweighting techniques fail [3, 14, 19, 4]. Because the path measures of the processes defined by \mathbf{X}_t and \mathbf{X}_t^{ϵ} are mutually singular, a straightforward application of the Girsanov theorem cannot be carried out [20]. There is, however, a simple and surprisingly convenient remedy.

To build a stochastic process that can be reweighted relative to (1), we let $\Sigma(\mathbf{x}, t) = \sigma(\mathbf{x}, t)\tilde{\sigma}^T(\mathbf{x}, t) + \sigma^T(\mathbf{x}, t)\tilde{\sigma}(\mathbf{x}, t)$ and consider instead the SDE,

$$d\mathbf{X}_t^s = \left[\mathbf{b}(\mathbf{X}_t^s, t) - \frac{\epsilon}{2} ((\Sigma(\mathbf{X}_t^s, t)s(\mathbf{X}_t^s, t) + \nabla : \Sigma(\mathbf{X}_t^s, t))) \right] dt + \sigma(\mathbf{X}_t^s, t)d\mathbf{W}_t, \quad (4)$$

and we use the notation $[\nabla : \mathbf{G}]_i = \sum_j \frac{\partial}{\partial x_j} G_{ij}$ and $\nabla \nabla : \mathbf{G} = \sum_{ij} \frac{\partial^2}{\partial x_i \partial x_j} G_{ij}$ to denote the double dot products of a differential operator with a dyadic tensor [21]. The solution of the associated Fokker-Planck equation,

$$\partial_t \rho_t^s = -\nabla \cdot [(\mathbf{b}(\cdot, t)\rho_t^s] + \frac{1}{2} \nabla \nabla : [(D + \epsilon \Sigma)\rho_t^s] \quad (5)$$

with $D(\mathbf{x}, t) = \sigma(\mathbf{x}, t)\sigma^T(\mathbf{x}, t)$ defines s , the “score” function that appears in (4),

$$s(\mathbf{x}, t) = \nabla_{\mathbf{x}} \log \rho_t^s(\mathbf{x}). \quad (6)$$

In App. A, we show that ρ_t^s has controlled error to first order in $\epsilon \rightarrow 0$ compared with the solution ρ_t^{ϵ} of the Fokker-Planck equation of the original, perturbed dynamics (3), which solves

$$\partial_t \rho_t^{\epsilon} = -\nabla \cdot [(\mathbf{b}(\cdot, t)\rho_t^{\epsilon}] + \frac{1}{2} \nabla \nabla : [\tilde{D}\rho_t^{\epsilon}], \quad (7)$$

with $\tilde{D}(\mathbf{x}, t) = (\sigma(\mathbf{x}, t) + \epsilon \tilde{\sigma}(\mathbf{x}, t))(\sigma(\mathbf{x}, t) + \epsilon \tilde{\sigma}(\mathbf{x}, t))^T$. In particular, this allows us to compute the sensitivity of an observable A with respect to a perturbation using expectations over the modified process (4), i.e.,

$$\partial_{\tilde{\sigma}} A_t = \lim_{\epsilon \rightarrow 0} \epsilon^{-1} [\langle A(t) \rangle_s - \langle A(t) \rangle]. \quad (8)$$

Conveniently, this new process is constructed so that path reweighting relative to the original dynamics (1) using Girsanov can be carried out. A straightforward expansion to first order in ϵ yields,

$$\begin{aligned}\langle A(t) \rangle_s &= \left\langle A(t) \frac{d\mathbb{P}^s}{d\mathbb{P}} \right\rangle \\ &= \left\langle A(t) \exp \left[-\epsilon \int_0^T \sigma(\mathbf{X}_u, u)^{-1} F(\mathbf{X}_u, u) d\mathbf{W}_u + \frac{\epsilon^2}{2} \int_0^T \|\sigma(\mathbf{X}_u, u)^{-1} F(\mathbf{X}_u, u)\|^2 du \right] \right\rangle \quad (9) \\ &\stackrel{\epsilon \rightarrow 0}{=} \langle A(t) \rangle - \epsilon \left\langle A(t) \int_0^T \sigma(\mathbf{X}_u, u)^{-1} F(\mathbf{X}_u, u) d\mathbf{W}_u \right\rangle + \mathcal{O}(\epsilon^2),\end{aligned}$$

and

$$F(\mathbf{x}, t) \stackrel{\epsilon \rightarrow 0}{=} \frac{1}{2} (\Sigma(\mathbf{x}, t) s^0(\mathbf{x}, t) + \nabla : \Sigma(\mathbf{x}, t)) + \mathcal{O}(\epsilon^2), \quad (10)$$

where s^0 is the score of the instantaneous distribution of (1). Our main result is a simple expression for the sensitivity to an arbitrary perturbation in the diffusivity,

$$\partial_{\tilde{\sigma}} A_t = -\frac{1}{2} \left\langle A(t) \int_0^t \sigma(\mathbf{X}_u, u)^{-1} [\Sigma(\mathbf{X}_u, u) s^0(\mathbf{X}_u, u) + \nabla : \Sigma(\mathbf{X}_u, u)] d\mathbf{W}_u \right\rangle, \quad (11)$$

which can be computed along the dynamics of the unperturbed process \mathbf{X}_t . We emphasize that the formula (11) is extremely general, valid for both equilibrium and nonequilibrium dynamics, and making no assumptions of stationarity. For both overdamped and underdamped equilibrium dynamics, we show that making use of the explicit score in (11) recovers the fluctuation-dissipation theorem (FDT). However, for general non equilibrium systems, we must approximate the unknown score. We leverage recent breakthroughs in machine learning that have led to robust strategies for estimating the score from data [16–18] and provide a route to computing sensitivities for nonequilibrium systems. In what follows, we demonstrate the numerical and analytical validity of the estimator in a variety of examples, and highlight excellent performance in comparison with FDTs, finite differencing and explicit Malliavin sensitivities.

Numerical examples.— We begin by using (11) to evaluate the sensitivity of an equilibrium Gibbs-Boltzmann distribution to a perturbation in the temperature T , i.e.,

$$d\mathbf{X}_t = -\nabla U(\mathbf{X}_t) dt + \sqrt{2(T + \delta T)} d\mathbf{W}_t \quad (12)$$

with $X_0 \sim \rho_{\text{eq}}(\mathbf{x}) \propto \exp[-U(\mathbf{x})/T]$. ^{*} Making use of the general sensitivity formula (11) and the explicit unperturbed score $s^0(\mathbf{x}, t) = -\nabla U(\mathbf{x})/T$ we obtain the equilibrium sensitivity

$$\partial_{\tilde{\sigma}} A_t = \frac{1}{\sqrt{2T^3}} \left\langle A(t) \int_0^t \nabla U(\mathbf{X}_s) d\mathbf{W}_s \right\rangle. \quad (13)$$

We show in App. B that the overdamped equilibrium sensitivity (13) is equivalent to the standard fluctuation dissipation relation [22, 19]

$$\frac{1}{\sqrt{2T^3}} \left\langle A(t) \int_0^t \nabla U(\mathbf{X}_s) d\mathbf{W}_s \right\rangle = \frac{1}{T^2} [\langle AU \rangle - \langle A(t) U(0) \rangle]. \quad (14)$$

Extending the equilibrium sensitivity (13) to perturbed underdamped equilibrium dynamics with friction coefficient γ is straightforward and the temperature sensitivity is given in App. B.

As an illustration, we consider an underdamped equilibrium system of 7 interacting Lennard-Jones particles with pairwise interaction potential $U_{\text{LJ}}(r) = 4\epsilon \left[\left(\frac{\sigma}{r}\right)^{12} - \left(\frac{\sigma}{r}\right)^6 \right]$ confined in a simple harmonic potential $U_{\text{el}}(\mathbf{x}) = (\mathbf{x} \cdot \mathbf{x})/2$. We display on Fig. 1 the finite-time sensitivity of the particle-averaged hexatic order parameter

^{*}To first order in $\delta T \equiv \epsilon$, this is strictly equivalent to evaluating the sensitivity $\partial_{\tilde{\sigma}} A_t$ of the perturbed SDE $d\mathbf{X}_t = -\nabla U(\mathbf{X}_t) dt + (\sigma + \epsilon \tilde{\sigma}) d\mathbf{W}_t$ where $\sigma(\mathbf{x}, t) = \sqrt{2T}$ and $\tilde{\sigma}(\mathbf{x}, t) = 1/(\sqrt{2T})$ are simple scalars.

$$\phi_6(\mathbf{x}) = \frac{1}{7} \sum_{i=1}^7 \left| \sum_{j \neq i} e^{6i\theta_{ij}} \right| \quad (15)$$

and compare the underdamped score based sensitivity (47) to both finite difference and fluctuation dissipation estimates of the thermal sensitivity of ϕ_6 at a fixed time, $\partial_T \phi_6(t=1)$. Note that we observe good agreement over a range of temperatures spanning both typical ordered (low T) and disordered (high T) states.

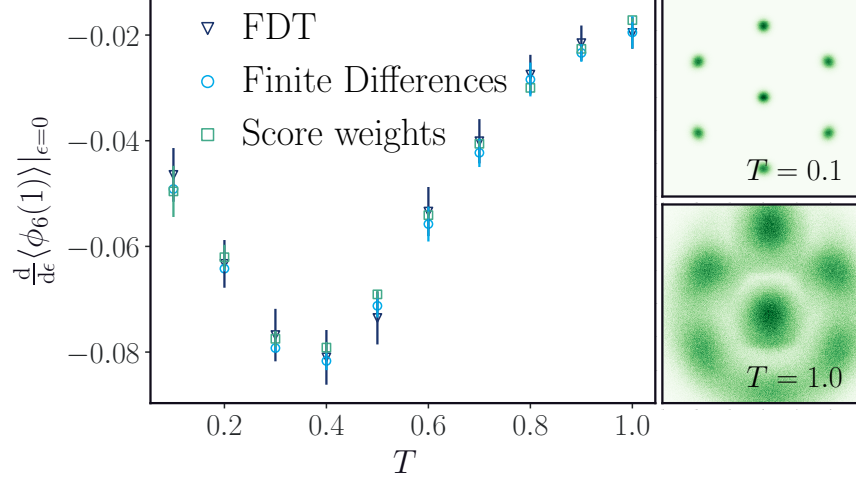


Figure 1: Temperature response for 7 Lennard-Jones interacting particles ($\sigma = 2.0$, $\epsilon = 1.0$) in a harmonic confining trap. We compute the sensitivity of the ϕ_6 order parameter at $t = 1$ after turning the perturbation on. The FDT, finite difference and score sensitivity estimates are respectively averaged over 10^6 , 4.10^6 and 2.10^7 samples. Right panel : aligned histograms for high and low temperatures. The hexatic nature of order is most present at low T , while diffusion prevails at high T .

Perturbing around a nonequilibrium steady-state.— For a general nonequilibrium steady-state (NESS) system, the FDT breaks down and a lack of explicit form for the stationary distribution of the system prevents direct evaluation of static sensitivities. Recent progress on score-estimation using flexible neural networks [16–18] has enabled computation of $\nabla \log \rho_{ss}$ for nonequilibrium distributions that were previously intractable. Leveraging these algorithms allows us to build a precise representation of the NESS score which, together with the score sensitivity formula (11) constitute unbiased estimators of diffusion sensitivities.

As an illustration, we consider in the following a four dimensional NESS system initially introduced in [17] and closely follow their notations for clarity. The system is composed of two one-dimensional interacting active particles on a ring of size L whose positions x^i and orientations g^i evolve according to the coupled SDEs,

$$\begin{aligned} dx_t^i &= [\mu f(x_t^i - x_t^j) + v_0 g_t^i] dt + \sqrt{2T} dW_t^{i,x} \\ dg_t^i &= -\gamma g_t^i dt + \sqrt{2\gamma} dW_t^{i,g} \end{aligned} \quad (16)$$

where $W_t^{i,k}$ and $W_s^{j,l}$ are independent Wiener processes. The soft repulsive interaction kernel is given by

$$f(x) = \frac{x}{\alpha|x|} \log(1 + \exp(\alpha(2r - |x|))), \quad (17)$$

where α and r are parameters accounting respectively for the intensity and cutoff distance of the interaction. Because of periodicity, the system is fully described by the reduced variables $x_t = x_t^1 - x_t^2$, $g_t = g_t^1 - g_t^2$ and

the corresponding dynamics

$$\begin{aligned} dx_t &= [2\mu f(x_t) + v_0 g_t] dt + 2\sqrt{T} dW_t^x \\ dg_t &= -\gamma g_t dt + 2\sqrt{\gamma} dW_t^g, \end{aligned} \quad (18)$$

where W_t^i and W_t^j are independent Wiener processes. As discussed in depth in [17], the variable (x_t, g_t) reaches a NESS (see Fig. 2), whose unknown stationary distribution ρ_{ss} depends on the temperature T .

To make use of the sensitivity formula (11), we represent the stationary score s^0 with a neural network trained on stationary data (see App. C.1 for training details), and we numerically evaluate the static sensitivity of the variance $\langle x^2 \rangle$ of the reduced system (18) with respect to a change in temperature T , as shown in Fig. 2. The measured sensitivity agrees within error to both an estimate via finite differences and also by numerical solution of the associated Fokker-Planck equation. This agreement holds across a range of temperatures, but higher estimation errors at lower T arise due to stronger gradients of ρ_{ss} (see right panel of Fig 2), which are computationally more difficult to represent.

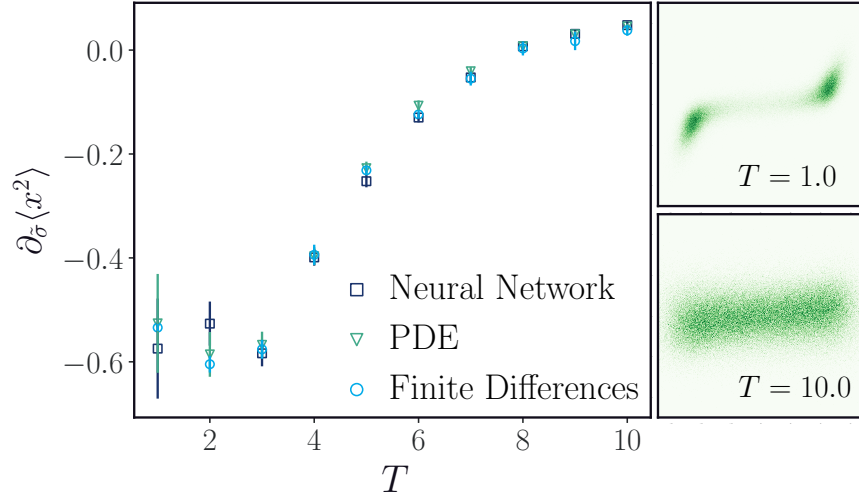


Figure 2: Static temperature response of the stationary variance associated to the distance between two interacting active particles on a ring. The finite difference, neural network and numerical solution estimates of the variance sensitivity are respectively averaged over 10^6 , 10^6 and $4 \cdot 10^6$ samples. Right panel : histograms in the (x, g) plane for high and low temperatures. Probability localization is most present at low T , while diffusion prevails at high T .

Nonequilibrium non-stationary dynamics.— While stationarity is a typical assumption for physical perturbation theories, there are many settings that occasion computing sensitivities for non-stationary dynamics. Specifically, throughout the financial risk literature, diffusion sensitivities are studied for their implications in options pricing, often using the Malliavin calculus. Our framework applies directly to the non-stationary setting, though we expect that learning a non-stationary score function for an arbitrary dynamics will be computationally challenging. As a proof of concept, we apply the score sensitivity formula (11) to evaluate diffusion sensitivities associated with variations of the volatility σ , or *vega* [15], in the celebrated one-dimensional Black-Scholes [23] model, which is defined by the stochastic differential equation

$$dX_t = \mu X_t dt + \sigma X_t dW_t; \quad X_0 = 1. \quad (19)$$

Because the solution to (19) is an exponential Brownian Motion $X_t = \exp\left[\left(\mu - \frac{\sigma^2}{2}\right)t + \sigma W_t\right]$, the unperturbed dynamical score is explicitly given by $s^0(x, t) = -\frac{3}{2x} + \frac{\mu}{x\sigma^2} - \frac{\log(x)}{\sigma^2 t x}$. In the score sensitivity formula (11), the volatility sensitivity *vega* corresponds to $\partial_{\tilde{\sigma}} A_t$ with $\tilde{\sigma}(x) = x$ and we immediately obtain

$$\partial_{\tilde{\sigma}} A_t = \left\langle A(t) \left[\int_0^t \frac{W_s}{\sigma s} dW_s - W_t \right] \right\rangle. \quad (20)$$

We prove in App. D that the score sensitivity (20) is equal to the Malliavin *vega* [15]

$$\left\langle A(t) \left[\frac{W_t^2}{\sigma t} - W_t - \frac{1}{\sigma} \right] \right\rangle, \quad (21)$$

and numerically compare both estimates of $\partial_{\bar{\sigma}} \langle X_t^2 \rangle$ on Fig. 3. Our estimate (20) is in perfect agreement with both the Malliavin result and the explicit analytical sensitivity.

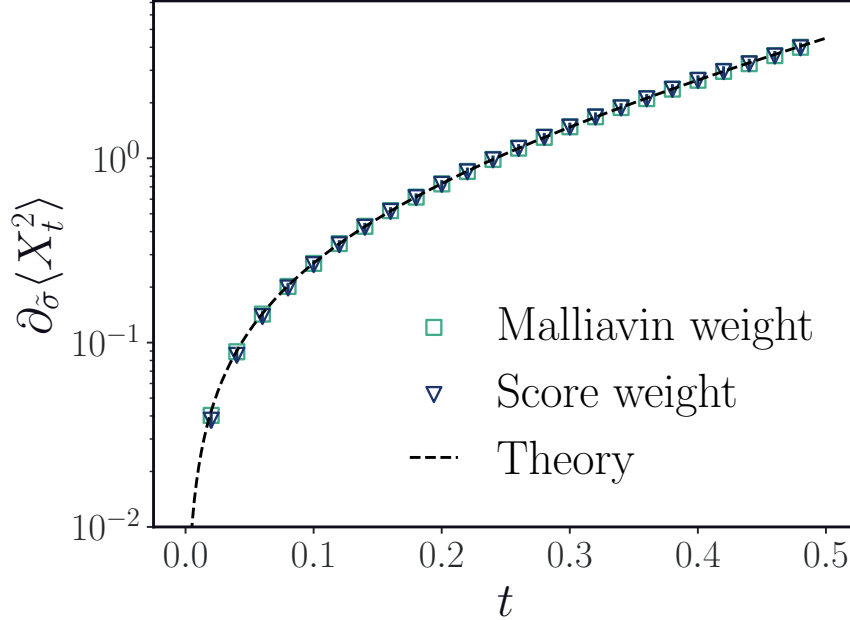


Figure 3: Black-Scholes model with $\mu = 1, \sigma = 1$; time dependent *vega* of the second moment $\partial_{\bar{\sigma}} \langle X_t^2 \rangle$. Both Malliavin and score estimates are averaged over $4 \cdot 10^5$ sample trajectories. The dashed analytical line is given in App. D.

Conclusions.— Predicting the response of a nonequilibrium physical system to an externally imposed change can elucidate subtle, dynamical fluctuations that underlie the sensitive and surprising adaptability of nanoscale systems. The challenge of carrying out these calculations in physical systems of interest, however, has led to a variety of different approaches that are not applicable in every setting. The general methodology that we have introduced enables us to leverage new computational tools from machine learning to compute the response to a perturbation in the diffusion tensor of a stochastic dynamics. For equilibrium systems, the score that appears in (11) is given exactly in terms of the potential energy and we recover the classical fluctuation dissipation theorem. For nonequilibrium systems, both at stationarity and otherwise, the score can be estimated and represented with a neural network. Approximating the score in this way gives excellent results on a variety of systems and offer considerable flexibility when compared with the Malliavin approach.

Examining the score-perturbed SDE (4) leads to a clear physical picture of the effective process: the additional drift in this equation acts as a force to enhance or suppress the variance of the instantaneous distribution, depending on the nature of the perturbation. While we have shown that this strategy exactly coincides with the Malliavin approach for the important case of Black-Scholes, a more general proof of equivalence remains. Because the framework that we have introduced simplifies computations of gradients with respect to the diffusivity for an arbitrary SDE, it also enables optimization, which we anticipate will be useful in the general machine learning context.

A Controlling the error between the score-shifted and the perturbed processes

In this appendix, we formally analyze the discrepancy between the score-shifted process and the exactly perturbed process. We make assumptions that lead to well-posed partial differential equations, for example, we assume the assumption of a uniformly parabolic diffusion tensor.

Assumption A.1 *The drift and mobility functions $\mathbf{b}_i, \sigma_{ij}, \tilde{\sigma}_{ij}$ are elements of the function space $L^\infty(\Omega)$.*

Assumption A.2 *For all $\epsilon > 0$ and $\boldsymbol{\xi} \in \mathbb{R}^d$ the mobility function $\sigma : \Omega \rightarrow \mathbb{R}^d$ and the perturbation $\tilde{\sigma} : \Omega \rightarrow \mathbb{R}^d$ satisfy the inequality*

$$\boldsymbol{\xi}^T \tilde{\mathbf{D}} \boldsymbol{\xi} \geq \tilde{C} \|\boldsymbol{\xi}\|^2 \quad (22)$$

for some constant $C > 0$ with $\tilde{\mathbf{D}}(\mathbf{x}, t) = (\sigma(\mathbf{x}, t) + \epsilon \tilde{\sigma}(\mathbf{x}, t))(\sigma(\mathbf{x}, t) + \epsilon \tilde{\sigma}(\mathbf{x}, t))^T$. And an analogous statement holds for \mathbf{D} alone with constant C .

The perturbed process

$$d\mathbf{X}_t^\epsilon = \mathbf{b}(\mathbf{X}_t^\epsilon, t)dt + [\sigma(\mathbf{X}_t^\epsilon, t) + \epsilon \tilde{\sigma}(\mathbf{X}_t^\epsilon, t)] d\mathbf{W}_t, \quad (23)$$

has a corresponding Fokker-Planck equation

$$\begin{aligned} \partial_t \rho_t^\epsilon &= -\nabla \cdot [(\mathbf{b}(\cdot, t) \rho_t^\epsilon] + \frac{1}{2} \nabla \nabla : [\tilde{\mathbf{D}}(\cdot, t) \rho_t^\epsilon], \\ &:= \mathcal{L}^\epsilon \rho_t^\epsilon \end{aligned} \quad (24)$$

with $\tilde{\mathbf{D}}(\mathbf{x}, t) = (\sigma(\mathbf{x}, t) + \epsilon \tilde{\sigma}(\mathbf{x}, t))(\sigma(\mathbf{x}, t) + \epsilon \tilde{\sigma}(\mathbf{x}, t))^T$.

Our goal is to establish a notion of equivalence between the aforementioned perturbed process and the score-shifted process. Recalling the definition $\Sigma(\mathbf{x}, t) = \sigma(\mathbf{x}, t) \tilde{\sigma}^T(\mathbf{x}, t) + \sigma^T(\mathbf{x}, t) \tilde{\sigma}(\mathbf{x}, t)$, the score-shifted SDE is

$$d\mathbf{X}_t^s = \left[\mathbf{b}(\mathbf{X}_t^s, t) - \frac{\epsilon}{2} ((\Sigma(\mathbf{X}_t^s, t) s(\mathbf{X}_t^s, t) + \nabla : \Sigma(\mathbf{X}_t^s, t)) \right] dt + \sigma(\mathbf{X}_t^s, t) d\mathbf{W}_t, \quad (25)$$

where $[\nabla : \mathbf{G}]_i = \sum_j \frac{\partial}{\partial x_j} G_{ij}$ and $\nabla \nabla : \mathbf{G} = \sum_{ij} \frac{\partial^2}{\partial x_i \partial x_j} G_{ij}$. The solution of the associated Fokker-Planck equation,

$$\partial_t \rho_t^s = -\nabla \cdot [(\mathbf{b}(\cdot, t) - \frac{\epsilon}{2} ((\Sigma(\cdot, t) s(\cdot, t) + \nabla : \Sigma(\cdot, t)) \rho_t^s] + \frac{1}{2} \nabla \nabla : [\mathbf{D}(\cdot, t) \rho_t^s] \quad (26)$$

with $\mathbf{D}(\mathbf{x}, t) = \sigma(\mathbf{x}, t) \sigma^T(\mathbf{x}, t)$ defines s , and the score is given by,

$$s(\mathbf{x}, t) = \nabla \log \rho_t^s(\mathbf{x}). \quad (27)$$

Using the fact that

$$\Sigma \nabla \log \rho + \nabla : \Sigma = \frac{\nabla : (\Sigma \rho)}{\rho}, \quad (28)$$

we deduce that

$$\partial_t \rho_t^s := \mathcal{L}^s \rho_t^s \equiv -\nabla \cdot [(\mathbf{b}(\cdot, t) \rho_t^s] + \frac{1}{2} \nabla \nabla : [(\mathbf{D} + \epsilon \Sigma) \rho_t^s]. \quad (29)$$

Let $\chi : \Omega \rightarrow \mathbb{R}$ be a test function. We are interested in the discrepancy

$$\begin{aligned} & \int_{\Omega} \chi(\mathbf{x}) (\rho_t^\epsilon(d\mathbf{x}) - \rho_t^s(d\mathbf{x})), \\ &= \int_0^t \int_{\Omega} \chi(\mathbf{x}) (\mathcal{L}^\epsilon \rho_\tau^\epsilon(d\mathbf{x}) - \mathcal{L}^s \rho_\tau^s(d\mathbf{x})) d\tau, \\ &= \int_0^t \int_{\Omega} \chi(\mathbf{x}) \left(\mathcal{L}^s(\rho_\tau^\epsilon(d\mathbf{x}) - \rho_\tau^s(d\mathbf{x})) + \frac{\epsilon^2}{2} \nabla \nabla : [\tilde{\sigma} \tilde{\sigma}^T \rho_\tau^\epsilon] \right) d\tau, \\ &= \int_0^t \int_{\Omega} \chi(\mathbf{x}) \left(\left[\mathcal{L}^s + \frac{\epsilon^2}{2} \tilde{\mathcal{L}} \right] \rho_\tau^\epsilon(d\mathbf{x}) - \mathcal{L}^s \rho_\tau^s(d\mathbf{x}) \right) d\tau, \end{aligned} \quad (30)$$

where $\tilde{\mathcal{L}}$ is the diffusion operator with mobility $\tilde{\sigma}$. The formal solution of the discrepancy can be written in terms of the time-order exponential operators associated with the linear PDE operators, i.e.,

$$\delta\rho_t := \left(e^{t\left[\mathcal{L}^s + \frac{\epsilon^2}{2}\tilde{\mathcal{L}}\right]} - e^{t\mathcal{L}^s} \right) \rho_0 \equiv \rho_t^\epsilon - \rho_t^s. \quad (31)$$

Letting $\epsilon \rightarrow 0$, we use the expansion,

$$\delta\rho_t = \left(1 + \frac{\epsilon^2}{2}t\tilde{\mathcal{L}} \right) e^{t\mathcal{L}^s} \rho_0 - e^{t\mathcal{L}^s} \rho_0 \implies \delta\rho_t = \frac{\epsilon^2}{2}t\tilde{\mathcal{L}}e^{t\mathcal{L}^s} \rho_0 \quad (32)$$

In particular [24], for each time $t > 0$ there exists a constant $C_\Omega(t)$ depending only on t, Ω , and the coefficients of \mathcal{L}^s such that

$$\sup_{\tau \in [0, t]} \|\rho_t^s\| \leq C_\Omega(t) \|\rho_0\|_{L_2(\Omega)}. \quad (33)$$

In addition, the action of the linear operator $\tilde{\mathcal{L}}$ on the bounded density ρ_t^s remains bounded by assumption. Hence, for any time t we can choose $\epsilon > 0$ sufficiently small such that the scaled deviation

$$\epsilon^{-1} \int_{\Omega} \chi(\mathbf{x}) (\rho_t^\epsilon(\mathrm{d}\mathbf{x}) - \rho_t^s(\mathrm{d}\mathbf{x})) \quad (34)$$

remains order ϵ .

B Fluctuation dissipation theorem for overdamped equilibrium systems subject to temperature changes

In this self-contained section, we derive the fluctuation dissipation relation for overdamped equilibrium dynamics subject to a change in the temperature, and prove the equivalence to the score sensitivity (13). Without loss of generality, we consider the one-dimensional case

$$\mathrm{d}X_t = -\nabla U(X_t)\mathrm{d}t + \sqrt{2T}\mathrm{d}W_t \quad (35)$$

with $X_0 \sim \rho^0(x) \propto \exp[-U(x)/T]$. At $t = 0$, the temperature is perturbed to $T + \epsilon$. The instantaneous distribution ρ_t of X_t evolves according to the perturbed Fokker-Planck equation

$$\partial_t \rho_t = \mathcal{L} \rho_t + \epsilon \mathcal{L}^1 \rho_t \quad (36)$$

with $\mathcal{L}f = -\nabla[-\nabla U f] + T\Delta f$ and $\mathcal{L}^1 = \Delta$. Following [25], we expand $\rho_t = \rho_t^0 + \epsilon \rho_t^1 + \mathcal{O}(\epsilon^2)$ in powers of ϵ and solve (36) to each order:

$$\begin{aligned} \partial_t \rho_t^0 &= \mathcal{L} \rho_t^0 \\ \partial_t \rho_t^1 &= \mathcal{L} \rho_t^1 + \mathcal{L} \rho_t^0. \end{aligned} \quad (37)$$

The formal first order solution of (36) is then given by

$$\rho_t = \rho^0 + \epsilon \int_0^t e^{\mathcal{L}(t-s)} \mathcal{L}^1 \rho^0 + \mathcal{O}(\epsilon^2), \quad (38)$$

and sensitivities of bounded continuous observables read

$$\left. \frac{\mathrm{d}\langle A(t) \rangle}{\mathrm{d}\epsilon} \right|_{\epsilon=0} = \int_{\mathbb{R}} \mathrm{d}x A(x) \int_0^t e^{\mathcal{L}(t-s)} \mathcal{L}^1 \rho^0. \quad (39)$$

Next, it is clear that $\mathcal{L}^1 \rho^0 = -\beta^2(LU\rho^0)$, where $Lf = -\nabla U \nabla f + T\Delta f$ is the adjoint of \mathcal{L} and $\beta = T^{-1}$. In turn, denoting $\langle \cdot \rangle_0$ equilibrium expectations with respect to ρ_0 , the sensitivity (39) is rewritten as

$$\begin{aligned}
\left. \frac{d \langle A(t) \rangle}{d\epsilon} \right|_{\epsilon=0} &= -\beta^2 \int_0^t ds \int_{\mathbb{R}} dx L e^{L(t-s)} A(x) U(x) \rho^0 \\
&= \beta^2 \int_0^t ds \frac{d}{ds} \langle A(t) U(s) \rangle_0 \\
&= \beta^2 [\langle AU \rangle_0 - A(t) U_0]
\end{aligned} \tag{40}$$

and we recover the FDT (13). We now show that one obtains the same result from the score sensitivity

$$\partial_{\tilde{\sigma}} A_t = \frac{1}{\sqrt{2T^3}} \left\langle A(t) \int_0^t \nabla U(X_s) dW_s \right\rangle \tag{41}$$

with $\tilde{\sigma} = 1/\sqrt{2T}$. Using Itô calculus, we first compute the total differential of $U(X_t)$

$$dU(X_t) = \nabla U(X_t) dX_t + \frac{1}{2} \Delta U(X_t) dt = \nabla U(X_t) [-\nabla U(X_t) dt + \sqrt{2T} dW_t] + T \Delta U(X_t) dt, \tag{42}$$

such that

$$\sqrt{2T} \int_0^t \nabla U(X_s) dW_s = U(X_t) - U(X_0) + \int_0^t [(\nabla U)^2 - T \Delta U] ds \tag{43}$$

where we recognize once again the generator L applied to the potential U

$$\frac{1}{\sqrt{2T^3}} \int_0^t \nabla U(X_s) dW_s = \frac{1}{2T^2} \left[U(X_t) - U(X_0) - \int_0^t L U ds \right]. \tag{44}$$

Using shorthand notations $B_s = B(X_s)$, we then obtain :

$$\begin{aligned}
\partial_{\tilde{\sigma}} A_t &= \frac{1}{\sqrt{2T^3}} \left\langle A(t) \int_0^t \nabla U(X_s) dW_s \right\rangle \\
&= \frac{1}{2T^2} \left[\langle A_t U_t \rangle - \langle A_t U_0 \rangle - \int_0^t \langle A_t L U_s \rangle ds \right] \\
&= \frac{1}{2T^2} \left[\langle A_t U_t \rangle - \langle A_t U_0 \rangle + \int_0^t \frac{d}{ds} \langle A_t U_s \rangle ds \right] \\
&= \frac{1}{2T^2} [\langle A_t U_t \rangle - \langle A_t U_0 \rangle + [\langle A_t U_t \rangle - \langle A_t U_0 \rangle]] \\
&= \frac{1}{T^2} [\langle AU \rangle - \langle A_t U_0 \rangle]
\end{aligned} \tag{45}$$

and recover the FDT (40). For perturbed underdamped equilibrium dynamics

$$\begin{aligned}
d\mathbf{X}_t &= \mathbf{V}_t dt, \\
d\mathbf{V}_t &= [-\nabla U(\mathbf{X}_t) - \gamma \mathbf{V}_t] dt + \sqrt{2\gamma(T + \epsilon)} d\mathbf{W}_t,
\end{aligned} \tag{46}$$

where \mathbf{X}_t and \mathbf{V}_t describe the system's instantaneous positions and momenta, only the momenta part of the score $\nabla_{\mathbf{v}} \rho_{\text{eq}}(\mathbf{x}, \mathbf{v}) = -\mathbf{v}/T$ is relevant to compute temperature sensitivities, and, in that case, the general formula (11) reads

$$\partial_{\tilde{\sigma}} \langle A_t \rangle = \frac{\gamma^{\frac{1}{2}}}{\sqrt{2T^3}} \left\langle A(t) \int_0^t \mathbf{V}_s d\mathbf{W}_s \right\rangle, \tag{47}$$

with $\tilde{\sigma} = 1/\sqrt{2\gamma T}$.

C Interacting active particles

In this section, we provide details on the numerical implementation of the non equilibrium steady state system (18). In particular, we discuss the neural network (NN) representation and the numerical estimate of the stationary distribution. We also gather here the values of parameters appearing in the dynamics (18) and used throughout : $L = 10, \mu = 10, v_0 = 5, \gamma = 0.1, \alpha = 7.5, r = 1.0$. Finally, note that in the sensitivity framework (11), static sensitivities to temperature variations for arbitrary observable A correspond to $\partial_{\tilde{\sigma}} A$ with

$$\tilde{\sigma} = \begin{pmatrix} 1/\sqrt{T} & 0 \\ 0 & 0 \end{pmatrix}. \quad (48)$$

C.1 Training details

Since the NESS score s^0 is not analytically tractable, we use a neural network (NN) representation \hat{s} trained on stationary simulation data, and minimize the agnostic/Fokker-Planck composite objective [17]

$$\mathcal{L}[\hat{s}] = \mathbb{E}_{\rho_{ss}} [|\hat{s}|^2 + 2\nabla\hat{s}] + \mathbb{E}_{\rho_{ss}} [(\nabla\hat{v} + \hat{v}\hat{s})^2]. \quad (49)$$

Loss function. We first comment on the composite loss (49) used as an objective for the score \hat{s} . While the first term of the right hand side is the agnostic Hyvärinen [18] score loss, the second term has first been introduced in [17] to take into account the dynamics of the system. Specifically, for Fokker Planck dynamics

$$\partial_t \rho_t = -\nabla[\mathbf{b}\rho] + \frac{1}{2}\nabla\nabla : [\mathbf{D}\rho_t] \quad (50)$$

with space and time independent \mathbf{D} and time independent \mathbf{b} , the stationary score s^0 is shown to satisfy the following ODE:

$$\nabla \cdot v + v \cdot s^0 = 0, \quad v = \mathbf{b} - \frac{\mathbf{D}}{2} s^0. \quad (51)$$

In turn, the objective (49) penalizes deviations from zero of the residual $\nabla\hat{v} + \hat{v}\hat{s}$, where $\hat{v} = \mathbf{b} - \frac{\mathbf{D}}{2}\hat{s}$.

Training protocol. For each temperature T in Fig. 2, we represent $\hat{s} : \mathbb{R}^2 \rightarrow \mathbb{R}^2$ as a fully connected NN with 4 layers, 256 hidden nodes and GELU activation function. The objective (49) is minimized on a training set of 10^5 equilibrated samples obtained from simulation of the dynamics (18). We use the Adam [26] optimizer with learning rate $\ell = 10^{-5}$, batch size 1024 and 100 learning epochs (10^5 learning steps).

Sensitivity estimation The static score sensitivity $\partial_{\tilde{\sigma}} \langle x^2 \rangle$ is averaged over 10^6 trajectories of duration $t = 4$ and time step $dt = 10^{-3}$.

C.2 Numerical solution to the Fokker Planck equation

Because of the low dimensionality of the SDE (18), we numerically solve the associated Fokker Planck equation

$$\partial_t \rho_t(x, g) = -\partial_x [(2\mu f(x) + v_0 g)\rho_t(x, g)] - \partial_g [(-\gamma g)\rho_t(x, g)] + [2T\partial_{xx} + 2\gamma\partial_{vv}] \rho_t(x, g) \quad (52)$$

to obtain an alternative score estimate. Note that we solve (52) on the finite domain $[-L/2, L/2]^2$ and impose periodic boundary conditions; this approximation provides satisfactory results since the true stationary marginal of g is a Gaussian with mean zero and variance 1. Because we know from simulation that the stationary distribution is bimodal (see figure 2), we initialize $\rho_{t=0}$ as a mixture of normal Gaussians centered at $(-L/4, 0)$ and $(L/4, 0)$ respectively. We use a pseudospectral integrator [27] on a grid of size (512×512) for $4 \cdot 10^4$ steps with time-step $dt = 10^{-4}$. The fast Fourier transforms and inverse transforms are carried out using the python package `numpy` [28]. Finally, we interpolate the discrete solution using `scipy`'s [29] `RegularGridInterpolator`, and evaluate the corresponding score.

Sensitivity estimation The static score sensitivity $\partial_{\sigma} \langle x^2 \rangle$ in Fig. 2 is averaged over 4×10^6 trajectories of duration $t = 4$ and time step $dt = 10^{-3}$.

D Malliavin Calculus for the Black-Scholes model

In this section we show that the score sensitivity $\left\langle A(X_t) \left[\int_0^t \frac{W_s}{\sigma s} dW_s - W_t \right] \right\rangle$ and Malliavin sensitivities (21) [13, 15] $\left\langle A(X_t) \left[\frac{W_t^2}{\sigma t} - W_t - \frac{1}{\sigma} \right] \right\rangle$ associated to variations of the volatility σ in the Black-Scholes model are equal for all bounded \mathcal{C}^1 observables $A : \mathbb{R} \rightarrow \mathbb{R}$ and $t > 0$, where the average is taken over the non stationary dynamics

$$dX_t = \mu X_t dt + \sigma X_t dW_t; \quad X_0 = 1. \quad (53)$$

Malliavin duality formula. A thorough discussion on Malliavin calculus is well beyond the scope of this paper. However, we still need to introduce a few notations in order to prove that

$$\left\langle A(X_t) \left[\frac{W_t^2}{\sigma t} - W_t - \frac{1}{\sigma} \right] \right\rangle = \left\langle A(X_t) \left[\int_0^t \frac{W_s}{\sigma s} dW_s - W_t \right] \right\rangle. \quad (54)$$

First, denoting $(\mathcal{F}_t)_{t \geq 0}$ the natural Brownian filtration associated to W_t , the Malliavin duality formula relates product expectations $\left\langle A_t \int_0^t v_s dW_s \right\rangle$ of $(\mathcal{F}_t)_{t \geq 0}$ measurable processes A_t and v_t to the “Malliavin derivative” $D_s [A(X_t)]$ in the following sense

$$\left\langle A(X_t) \int_0^t v_s dW_s \right\rangle = \left\langle \int_0^t ds D_s [A(X_t)] v_s \right\rangle. \quad (55)$$

The Malliavin derivative is itself a complicated stochastic process which often does not have an explicit form. However, In the Black-Scholes case (53), it is a.s. equal to

$$D_s [A(X_t)] = \sigma A'(X_t) X_t \quad (56)$$

for all $s \leq t$. We now make use of the duality formula (55) to rewrite the score sensitivity in terms of $A'(X_t)$. First

$$\begin{aligned} \left\langle A(X_t) \left[\int_0^t \frac{W_s}{\sigma s} dW_s - W_t \right] \right\rangle &= \left\langle A(X_t) \left[\int_0^t \left(\frac{W_s}{\sigma s} - 1 \right) dW_s \right] \right\rangle \\ &= \left\langle A(X_t) \left[\int_0^t dW_u \left(\int_u^t \frac{dW_s}{\sigma s} - 1 \right) \right] \right\rangle. \end{aligned} \quad (57)$$

We identify $v_u = \left(\int_u^t \frac{dW_s}{\sigma s} - 1 \right)$ and use the Malliavin duality formula along with (56) to obtain

$$\begin{aligned} \left\langle A(X_t) \left[\int_0^t \frac{W_s}{\sigma s} dW_s - W_t \right] \right\rangle &= \left\langle A'(X_t) \sigma X_t \int_0^t du \left(\int_u^t \frac{dW_s}{\sigma s} - 1 \right) \right\rangle \\ &= \left\langle A'(X_t) \sigma X_t \left(\int_0^t \frac{dW_s}{\sigma s} \int_0^s du - t \right) \right\rangle \\ &= \langle A'(X_t) X_t (W_t - \sigma t) \rangle \end{aligned} \quad (58)$$

Finally, we use the fact (see [13], chapter 6 for instance) that

$$\langle A'(X_t) X_t (W_t - \sigma t) \rangle = \left\langle A(X_t) \left[\frac{W_t^2}{\sigma t} - W_t - \frac{1}{\sigma} \right] \right\rangle \quad (59)$$

to conclude. We emphasize that this calculation leverages the specific explicit forms of both the score and Malliavin derivative associated to the Black-Scholes model. A more general statement to relate score and Malliavin sensitivities requires further investigation, and is left for future work.

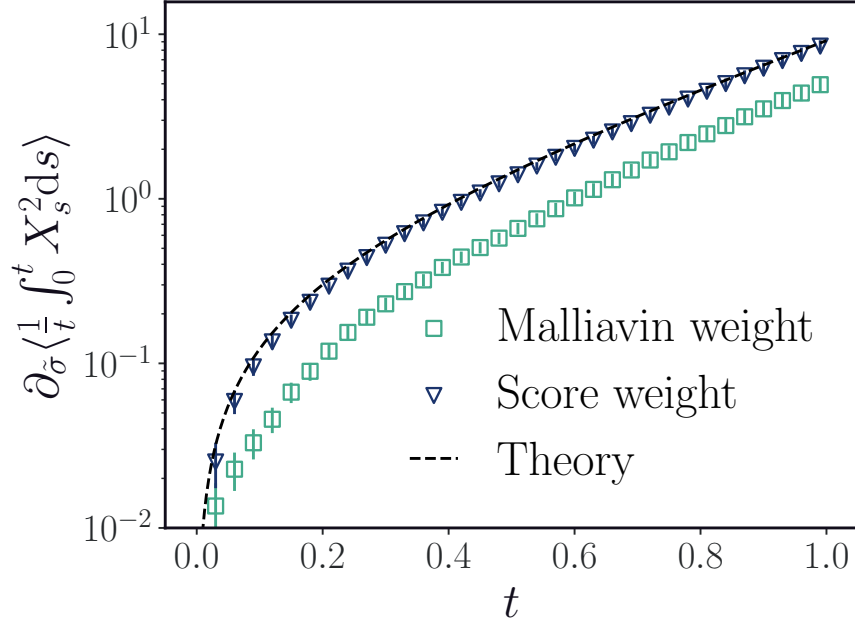


Figure 4: Black-Scholes model with $\mu = 1, \sigma = 1$; time dependent *vega* of the time integrated observable $A_t = \left[\frac{1}{t} \int_0^t X_s^2 ds \right]$. Both Malliavin and score estimates are averaged over $4 \cdot 10^5$ sample trajectories. Whereas the score estimate is in perfect agreement with the dashed analytical prediction (62), the Malliavin estimate (59) does not hold for time integrated observables.

Analytical sensitivity in Fig. 3. Since $X_t = \exp \left[\left(\mu - \frac{\sigma^2}{2} \right) t + \sigma W_t \right]$, the instantaneous distribution ρ_t of X_t is given by

$$\rho_t(x) = \exp \left[- \frac{\left[\log(x) - \left(\mu - \frac{\sigma^2}{2} \right) \right]^2}{2t\sigma^2} \right] / (\sqrt{2\pi\sigma^2 t} s), \quad (60)$$

and its second moment is explicit $\langle X_t^2 \rangle = e^{t(2\mu + \sigma^2)}$ such that

$$\partial_{\bar{\sigma}} \langle X_t^2 \rangle = 2t\sigma e^{t(2\mu + \sigma^2)}. \quad (61)$$

Integrated observables. We emphasize that the score sensitivity formula holds for time integrated observables $A(\{X_t\}_{t \geq 0})$ which depend on the full trajectory, without the need for any modifications. In contrast, the Malliavin formalism doesn't carry through as smoothly. We showcase that discrepancy in the Black-Scholes model by comparing the analytical sensitivity of the time integrated observable $A_t = \left[\frac{1}{t} \int_0^t X_s^2 ds \right]$

$$\partial_{\bar{\sigma}} A_t = \frac{2\sigma \left(e^{t(2\mu + \sigma^2)} (t(2\mu + \sigma^2) - 1) + 1 \right)}{(2\mu + \sigma^2)^2} \quad (62)$$

to the Malliavin estimate (59) and score estimate (11) on Fig. 4.

References

- [1] Lars Onsager. Reciprocal relations in irreversible processes. i. *Phys. Rev.*, 37:405–426, Feb 1931. doi: 10.1103/PhysRev.37.405. URL <https://link.aps.org/doi/10.1103/PhysRev.37.405>.

- [2] R Kubo. The fluctuation-dissipation theorem. *Rep. Prog. Phys.*, 29(1):255–284, 1966. doi: 10.1088/0034-4885/29/1/306. URL <http://stacks.iop.org/0034-4885/29/i=1/a=306?key=crossref.d8453ffc416cd2064d6ccd38e7c06a41>. tex.ids= kubo.fluctuation-dissipation_nodate.
- [3] C Maes, S Safaverdi, P Visco, and F van Wijland. Fluctuation-response relations for nonequilibrium diffusions with memory. *Phys. Rev. E*, 87(2):022125, February 2013. doi: 10.1103/PhysRevE.87.022125. URL <http://link.aps.org/doi/10.1103/PhysRevE.87.022125>.
- [4] Hyun-Myung Chun, Qi Gao, and Jordan M. Horowitz. Nonequilibrium Green-Kubo relations for hydrodynamic transport from an equilibrium-like fluctuation-response equality. *Physical Review Research*, 3(4):043172, December 2021. doi: 10.1103/PhysRevResearch.3.043172. URL <https://link.aps.org/doi/10.1103/PhysRevResearch.3.043172>. Publisher: American Physical Society.
- [5] Clemens Bechinger, Roberto Di Leonardo, Hartmut Löwen, Charles Reichhardt, Giorgio Volpe, and Giovanni Volpe. Active Particles in Complex and Crowded Environments. *Reviews of Modern Physics*, 88(4), November 2016. ISSN 0034-6861, 1539-0756. doi: 10/f3t6gr. URL <https://link.aps.org/doi/10.1103/RevModPhys.88.045006>.
- [6] Shriram Chennakesavalu and Grant M. Rotskoff. Probing the theoretical and computational limits of dissipative design. *The Journal of Chemical Physics*, 155(19):194114, November 2021. ISSN 0021-9606. doi: 10.1063/5.0067695. URL <http://aip.scitation.org/doi/10.1063/5.0067695>. Publisher: American Institute of Physics.
- [7] Aidan I. Brown and David A. Sivak. Theory of nonequilibrium free energy transduction by molecular machines. *Chemical Reviews*, 120(1):434–459, January 2020. ISSN 0009-2665, 1520-6890. doi: 10.1021/acs.chemrev.9b00254. URL <https://pubs.acs.org/doi/10.1021/acs.chemrev.9b00254>.
- [8] Eiji Yamamoto, Takuma Akimoto, Antreas C. Kalli, Kenji Yasuoka, and Mark S. P. Sansom. Dynamic interactions between a membrane binding protein and lipids induce fluctuating diffusivity. *Science Advances*, 3(1):e1601871, January 2017. doi: 10.1126/sciadv.1601871. URL <https://www.science.org/doi/10.1126/sciadv.1601871>.
- [9] Kay Brandner, Keiji Saito, and Udo Seifert. Thermodynamics of Micro- and Nano-Systems Driven by Periodic Temperature Variations. *Physical Review X*, 5(3):031019, August 2015. doi: 10.1103/PhysRevX.5.031019. URL <https://link.aps.org/doi/10.1103/PhysRevX.5.031019>. Publisher: American Physical Society.
- [10] Tushar K. Saha, Jannik Ehrich, Momčilo Gavrilov, Susanne Still, David A. Sivak, and John Bechhoefer. Information engine in a nonequilibrium bath. *Physical Review Letters*, 131(5):057101, August 2023. ISSN 0031-9007, 1079-7114. doi: 10.1103/PhysRevLett.131.057101. URL <https://journals.aps.org/prl/abstract/10.1103/PhysRevLett.131.057101>.
- [11] Gianmaria Falasco and Marco Baiesi. Temperature response in nonequilibrium stochastic systems. *Epl*, 113(2), 2016. ISSN 12864854. doi: 10.1209/0295-5075/113/20005. URL <https://iopscience.iop.org/article/10.1209/0295-5075/113/20005>. arXiv: 1509.03139.
- [12] Marco Baiesi, Urna Basu, and Christian Maes. Thermal response in driven diffusive systems. *The European Physical Journal B*, 87(11):277, November 2014. ISSN 1434-6028, 1434-6036. doi: 10.1140/epjb/e2014-50622-2. URL <https://link.springer.com/article/10.1140/epjb/e2014-50622-2>.
- [13] David Nualart. *The Malliavin Calculus and Related Topics*. Probability, its Applications. Springer-Verlag, Berlin/Heidelberg, 2006. ISBN 978-3-540-28328-7. doi: 10.1007/3-540-28329-3. URL <http://link.springer.com/10.1007/3-540-28329-3>.
- [14] Patrick B. Warren and Rosalind J. Allen. Malliavin Weight Sampling for Computing Sensitivity Coefficients in Brownian Dynamics Simulations. *Physical Review Letters*, 109(25):250601, December 2012. doi: 10.1103/PhysRevLett.109.250601. URL <https://link.aps.org/doi/10.1103/PhysRevLett.109.250601>. Publisher: American Physical Society.

- [15] Eric Fournié, Jean-Michel Lasry, Jérôme Lebuchoux, Pierre-Louis Lions, and Nizar Touzi. Applications of Malliavin calculus to Monte Carlo methods in finance. *Finance and Stochastics*, 3(4):391–412, 1999. ISSN 0949-2984. doi: 10.1007/s007800050068. URL <https://link.springer.com/article/10.1007/s007800050068>.
- [16] Yang Song, Jascha Sohl-Dickstein, Diederik P. Kingma, Abhishek Kumar, Stefano Ermon, and Ben Poole. Score-Based Generative Modeling through Stochastic Differential Equations. February 2022. URL <https://openreview.net/forum?id=PXTIG12RRHS>.
- [17] Nicholas M. Boffi and Eric Vanden-Eijnden. Deep learning probability flows and entropy production rates in active matter. pages 1–48, 2023. URL <http://arxiv.org/abs/2309.12991>. arXiv: 2309.12991.
- [18] Aapo Hyvärinen. Estimation of Non-Normalized Statistical Models by Score Matching. *Journal of Machine Learning Research*, 6(24):695–709, 2005. ISSN 1533-7928. URL <http://jmlr.org/papers/v6/hyvarinen05a.html>.
- [19] M. Baiesi and C. Maes. An update on the nonequilibrium linear response. *New Journal of Physics*, 15, 2013. ISSN 13672630. doi: 10.1088/1367-2630/15/1/013004. URL <https://iopscience.iop.org/article/10.1088/1367-2630/15/1/013004>. arXiv: 1205.4157.
- [20] Bernt Øksendal. *Stochastic Differential Equations*. Universitext. Springer Berlin Heidelberg, Berlin, Heidelberg, 2003. ISBN 978-3-540-04758-2 978-3-642-14394-6. doi: 10.1007/978-3-642-14394-6. URL <http://link.springer.com/10.1007/978-3-642-14394-6>.
- [21] Grigorios A. Pavliotis. *Stochastic Processes and Applications: Diffusion Processes, the Fokker-Planck and Langevin Equations*, volume 60 of *Texts in Applied Mathematics*. Springer New York, New York, NY, 2014. ISBN 978-1-4939-1322-0 978-1-4939-1323-7. doi: 10.1007/978-1-4939-1323-7. URL <http://link.springer.com/10.1007/978-1-4939-1323-7>.
- [22] Ryogo Kubo, Morikazu Toda, and Natsuki Hashitsume. *Statistical Physics II*, volume 31 of *Springer Series in Solid-State Sciences*. Springer, Berlin, Heidelberg, 1991. ISBN 978-3-540-53833-2 978-3-642-58244-8. doi: 10.1007/978-3-642-58244-8. URL <http://link.springer.com/10.1007/978-3-642-58244-8>.
- [23] Fischer Black and Myron Scholes. The pricing of options and corporate liabilities. *Journal of Political Economy*, 81(3):637–654, 1973. ISSN 00223808, 1537534X. URL <http://www.jstor.org/stable/1831029>.
- [24] Lawrence C. Evans. *Partial differential equations*. Number v. 19 in Graduate studies in mathematics. American Mathematical Society, Providence, R.I, 2nd ed edition, 2010. ISBN 978-0-8218-4974-3. OCLC: ocn465190110.
- [25] Robert Zwanzig. Nonlinear generalized Langevin equations. *Journal of Statistical Physics*, 9(3):215–220, November 1973. ISSN 0022-4715, 1572-9613. doi: 10.1007/BF01008729. URL <http://link.springer.com/10.1007/BF01008729>.
- [26] Diederik P. Kingma and Jimmy Ba. Adam: A method for stochastic optimization. In Yoshua Bengio and Yann LeCun, editors, *3rd International Conference on Learning Representations, ICLR 2015, San Diego, CA, USA, May 7-9, 2015, Conference Track Proceedings*, 2015. URL <http://arxiv.org/abs/1412.6980>.
- [27] Hector D. Ceniceros and Glenn H. Fredrickson. Numerical Solution of Polymer Self-Consistent Field Theory. *Multiscale Modeling & Simulation*, 2(3):452–474, January 2004. ISSN 1540-3459. doi: 10.1137/030601338. URL <https://epubs.siam.org/doi/abs/10.1137/030601338>. Publisher: Society for Industrial and Applied Mathematics.
- [28] Charles R. Harris, K. Jarrod Millman, Stéfán J. van der Walt, Ralf Gommers, Pauli Virtanen, David Cournapeau, Eric Wieser, Julian Taylor, Sebastian Berg, Nathaniel J. Smith, Robert Kern, Matti Picus, Stephan Hoyer, Marten H. van Kerkwijk, Matthew Brett, Allan Haldane, Jaime Fernández del Río, Mark

Wiebe, Pearu Peterson, Pierre Gérard-Marchant, Kevin Sheppard, Tyler Reddy, Warren Weckesser, Hameer Abbasi, Christoph Gohlke, and Travis E. Oliphant. Array programming with NumPy. *Nature*, 585(7825):357–362, September 2020. doi: 10.1038/s41586-020-2649-2. URL <https://doi.org/10.1038/s41586-020-2649-2>.

- [29] Pauli Virtanen, Ralf Gommers, Travis E. Oliphant, Matt Haberland, Tyler Reddy, David Cournapeau, Evgeni Burovski, Pearu Peterson, Warren Weckesser, Jonathan Bright, Stéfan J. van der Walt, Matthew Brett, Joshua Wilson, K. Jarrod Millman, Nikolay Mayorov, Andrew R. J. Nelson, Eric Jones, Robert Kern, Eric Larson, C J Carey, İlhan Polat, Yu Feng, Eric W. Moore, Jake VanderPlas, Denis Laxalde, Josef Perktold, Robert Cimrman, Ian Henriksen, E. A. Quintero, Charles R. Harris, Anne M. Archibald, Antônio H. Ribeiro, Fabian Pedregosa, Paul van Mulbregt, and SciPy 1.0 Contributors. SciPy 1.0: Fundamental Algorithms for Scientific Computing in Python. *Nature Methods*, 17:261–272, 2020. doi: 10.1038/s41592-019-0686-2. URL <https://rdcu.be/b08Wh>.